Inorganica Chimica Acta, 127 (1987) 141–146

Organomercury(II) Dithiocarbazates: Synthesis, Characterisation and Biological Studies

SANGEETA BHATIA, NARENDER K. KAUSHIK*

Department of Chemistry, University of Delhi, Delhi 110 007, India

and GURVINDER S. SODHI

Department of Chemistry, S.G.T.B. Khalsa College, University of Delhi, Delhi 110 007, India

(Received July 23, 1986)

Abstract

Organomercury(II) dithiocarbazate complexes of the type RHgL (I) and RHgL′ (II) [R = phenyl (C_6H_5), *o*-hydroxyphenyl (*o*-HOC_6H_4), *p*-hydroxyphenyl (*p*-HOC_6H_4), *p*-acetoxyphenyl (*p*-$AcOC_6H_4$), 2-furyl (2-C_4H_3O); L = phenyldithiocarbazate, L′ =

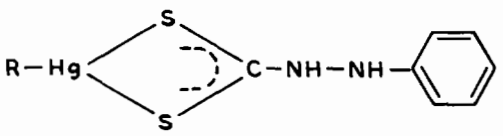

I

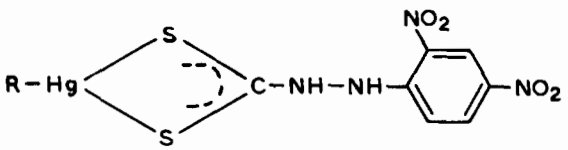

II

2,4-dinitrophenyldithiocarbazate] have been synthesised and characterised. Conductance measurements indicate that the compounds are non-electrolytes. From IR and UV spectral studies it is concluded that the dithiocarbazate moiety is bidentate. Fluorescence studies have been carried out for *o*-, *p*-HOC_6H_4HgL and *o*-, *p*-HOC_6H_4HgL' complexes and relevant photochemical parameters have been elucidated. For C_6H_5HgL, *p*-HOC_6H_4HgL, *p*-$AcOC_6H_4HgL$ and *p*-HOC_6H_4HgL' complexes, thermal studies (TG and DTA) have been carried out and kinetic and thermodynamic parameters for thermal degradation have been enumerated. In addition, the fragmentation patterns of the complexes have been analysed on the basis of mass spectra. The complexes show positive fungicidal and bactericidal activities.

*Author to whom correspondence should be addressed.

Introduction

The field of metal dithiocarbazates has grown from a primarily synthetic, exploratory stage to a more sophisticated stage where studies of reactivities, molecular structures and biochemical investigations are actively pursued. This is the outcome of the fact that the dithiocarbazate ligands exhibit many stereochemical and biochemical features [1–3]. Thus many new ligands have been designed to test various hypotheses regarding structural and medicinal properties, in particular antitumor activity of the complexes. With this aim we carried out the synthesis and characterisation of a number of organomercury(II) dithiocarbazates. This is in sequence to our investigation of metal ion–biomolecule interactions [4, 5].

Experimental

The following instruments were used: Elico conductivity Bridge, Model CM-82 for conductance measurements; Perkin-Elmer grating 621 spectrometer for IR spectra; Perkin-Elmer UV–Vis Spectrophotometer, model 554 for UV spectra; Jasco FP-550 spectrofluorometer for fluorescence studies; Shimadzu, Kyoto (Japan) Thermobalance for recording TG and DTA curves simultaneously in nitrogen atmosphere at a heating rate of 15° min^{-1}, with a chart speed of 5 mm min^{-1}. Mass spectra were recorded at the Central Drug Research Institute, Lucknow, India.

Nitrobenzene was purified for conductance measurements by the method of Fay *et al.* [6]. C_6H_5HgCl [7], *o*-, *p*-HOC_6H_4HgCl [8], *p*-$AcOC_6H_4HgCl$ [9] and 2-C_4H_3OHgCl [10] were prepared by standard methods.

Preparation of Ligands

Phenylhydrazinium phenyldithiocarbazate was prepared by the method of Anthoni [11]. Potassium

0020-1693/87/$3.50

TABLE I. Physical Characteristics and Elemental Analyses

Compound	Decomposition (°C)[a]	Λ^b ($C = 1.5 \times 10^{-3}$ M)	Analysis, found (calc.) (%)		
			Hg	S	N
C_6H_5HgL	120	0.46	43.68(43.55)	13.75(13.89)	6.18(6.07)
o-HOC_6H_4HgL	127	0.52	42.18(42.08)	13.30(13.42)	5.78(5.87)
p-HOC_6H_4HgL	105	0.58	41.96(42.08)	13.51(13.42)	5.97(5.87)
p-$AcOC_6H_4HgL$	118	0.50	38.76(38.67)	12.48(12.34)	5.49(5.39)
2-C_4H_3OHgL	114	0.46	45.06(44.51)	14.32(14.20)	6.18(6.21)
C_6H_5HgL'	133	0.48	36.31(36.43)	11.73(11.62)	10.03(10.17)
o-HOC_6H_4HgL'	178	0.52	35.52(35.40)	11.20(11.29)	9.72(9.88)
p-HOC_6H_4HgL'	135	0.56	35.53(35.40)	11.18(11.29)	9.99(9.88)
p-$AcOC_6H_4HgL'$	103	0.50	32.80(32.95)	10.65(10.51)	9.35(9.20)
2-C_4H_3OHgL'	122	0.48	37.21(37.10)	11.60(11.83)	5.28(5.17)

[a]Uncorrected values. [b]in ohm^{-1} cm^2 mol^{-1}.

2,4-dinitrophenyldithiocarbazate was prepared by dissolving 9.9 g (0.05 mol) 2,4-dinitrophenylhydrazine in a minimum quantity of anhydrous dimethylformamide and adding 2.8 g (0.05 mol) potassium hydroxide. To the stirred mixture, 3.8 ml (0.05 mol) carbon disulphide was added. After 1 h, a mixture of ethylacetate and petroleum ether (50 ml, 1:1 v/v) was added to the stirred contents and the product so obtained was filtered and dried.

Preparation of Complexes

A suspension of phenylhydrazinium phenyldithiocarbazate (0.05 mol) or potassium 2,4-dinitrophenyldithiocarbazate (0.05 mol) in 25 ml THF was slowly added to a solution of RHgCl (0.05 mol) in 25 ml THF. The contents were stirred for about 3 h and filtered. The filtrate was evaporated to one-fourth of its original volume and petroleum ether was added. The solid product separated out, was filtered and dried. It was recrystallised from acetone solution by the addition of petroleum ether.

Results and Discussion

The complexes are red or brown in colour. They are soluble in THF, DMSO and acetone. Conductance measurements reveal that compounds are non-electrolytes. From TLC and elemental analyses it is concluded that the compounds are pure. Some physical characteristics and elemental analysis data are presented in Table I.

IR Spectra

The evidence for S–S bonding in the complexes is provided by the N–H stretching frequencies. In the free ligand, the ν(N–H) stretching frequency is observed at 3150 cm^{-1}. If N–S bonding occurs, the ν(N–H) stretching frequency in the metal complexes should occur at lower frequencies than in free ligands. However, in the complexes under investigation the ν(N–H) is shifted to a higher frequency (~3300 cm^{-1}) which supports the inference of S–S bonding [12]. Further evidence for the S–S chelation is provided by the ν(C⋯S) stretching frequency. The criterion concerning the ν(C⋯S) stretching frequency as applied to dithiocarbamates [13] should be applicable to the dithiocarbazates too [14]. The free ligands show a doublet at 980 and 1005 cm^{-1} while the complexes exhibit a single strong band at ~1000 cm^{-1} which supports the inference of S–S bonding.

The IR spectra of metal complexes show a strong band in the 1350–1370 cm^{-1} region which is attributed to the ν(C⋯N) stretching frequency. In the free ligands the ν(C⋯N) frequency occurs at 1335 cm^{-1}. The occurrence of this frequency at lower energy in the free ligands as compared to the metal complexes is expected since on complexation there is an increase in electron density on the sulphur atoms due to back donation of electrons from metal d-orbitals to the vacant antibonding sulphur orbitals. This effect increases the (C⋯N) bond order. In the far infrared region the medium intensity bands are observed at ~360 cm^{-1} due to the ν(Hg–S) stretching frequency [15].

UV Spectra

In the UV region an intense band appears at *ca.* 226 nm (log ϵ ~ 4.35) due to the intraligand π–π^* transition of the N⋯C⋯S group [16–18]. The intraligand π–π^* transition of the S⋯C⋯S group generally appears as a shoulder band and is associated with the inequivalence of the C⋯S bonds of the ligand [19]. In the present compounds although this band is observed in the case of ligands at 322 nm (log ϵ 3.75), it tends to disappear in the case of metal complexes, showing thereby that the dithiocarbazate ligand is S–S bonded to the metal ions. This fact is in agreement with IR studies.

Fluorescence Studies

In the fluorescence spectra the absorption band is observed at *ca.* 228 nm (log ϵ ~ 3.5) while the emission

band is at *ca.* 455 nm. Thus, in accordance with the Franck–Condon principle and thermal relaxation of vibrational modes, the fluorescence spectra is observed on the red side of the absorption spectra in an approximately mirror image relationship [20]. In these complexes, however, the mirror image pattern is slightly disrupted with the appearance of a weak band at 313 nm ($\log \epsilon \sim 1.4$). The appearance of this band may be traced back to the fact that the coupling of electron spin and orbital angular momentum is strong in atoms like mercury [21]. Due to this the clear distinction between the singlet and triplet states breaks down; the singlet states have a partly triplet character and the triplet states a partly singlet character. The additional band thus arises due to the triplet → singlet transition, $Hg6(^3P_1) \rightarrow Hg6(^1S_0)$, which is forbidden by the rule prohibiting a change in multiplicity, $\Delta S = 0$. Not only is the $\Delta S = 0$ rule violated, but also the more stringent requirement that the transition $J = 0 \rightarrow J = 0$ is not allowed. As a result the 313 nm radiation is not absorbed by the mercury atom and it is not a resonance line. However, atoms in the $6(^3P_1)$ state can be collisionally deactivated to the $6(^3P_0)$ state, and if no reverse activation step occurs the atom will stay in this metastable state until it finally emits the forbidden 313 nm radiation and returns to the ground state [21]. The spectrum is free from anti-stokes effects. The pattern of the spectrum follows Levschin's rule, indicating that the geometry of the excited state is not very different from that of the ground state [22].

The actual radiative lifetime of the excited state, τ is smaller than the intrinsic radiative lifetime, τ_0, indicating the possibility of non-radiating energy dissipation processes depopulating the excited state. Thus, fluorescence remains the dominant but certainly not the exclusive mode of emission. The non-radiative processes, *i.e.* inter-system crossing and internal conversion, compete with fluorescence. Therefore, Einstein's probability of spontaneous absorption, B_{nm}, exceeds the corresponding probability of spontaneous emission, A_{mn}. The quantum yield of fluorescence, intersystem crossing and internal conversion follow the order $\phi_B > \phi_{ISC} > \phi_{IC}$. These priorities are also established by their respective rate constants [21].

The summation of rate constants for all the photochemical and photophysical processes competing with fluorescence, ΣK_i, equals the sum of K_{ISC} and K_{IC}. Thus apart from fluorescence, intersystem crossing and internal conversion, there seems to be no other mode of emission, radiative or non-radiative, in the present case [22]. The oscillator strength, f, has been calculated from the relation $f = 4.31 \times 10^{-9} \int \epsilon \bar{\nu}\, d\bar{\nu}$, which is valid if we assume a Lorenzian shape for the absorption band. The factor $\int \epsilon \bar{\nu}\, d\bar{\nu}$ is replaced by $\epsilon_{max}\ \Delta\bar{\nu}$ where $\Delta\bar{\nu}$ is the half band width of the absorption band [22]. The relevant data are presented in Table II.

TABLE II. Fluorescence Spectral Parameters

Parameter	*p*-HOC_6H_4HgL	*o*-HOC_6H_4HgL	*p*-HOC_6H_4HgL'	*o*-HOC_6H_4HgL'
Quantum yield of fluorescence: ϕ_f	0.88	0.78	0.80	0.87
Quantum yield for inter-system crossing: ϕ_{ISC}	0.11	0.21	0.19	0.12
Quantum yield for internal conversion: ϕ_{IC}	0.0034	0.0033	0.0033	0.0029
Oscillator strength: f	0.031	0.046	0.038	0.039
Actual radiative lifetime: τ (s)	3.07×10^{-8}	2.75×10^{-8}	2.75×10^{-8}	2.66×10^{-8}
Intrinsic radiative lifetime: τ_0 (s)	3.48×10^{-8}	3.52×10^{-8}	3.43×10^{-8}	3.05×10^{-8}
Rate constant of fluorescence emission: K_f (s^{-1})	0.28×10^8	0.28×10^8	0.29×10^8	0.32×10^8
Rate constant for intersystem crossing: K_{ISC} (s^{-1})	0.038×10^8	0.078×10^8	0.072×10^8	0.047×10^8
Rate constant for internal conversion: K_{IC} (s^{-1})	0.0011×10^8	0.0012×10^8	0.0012×10^8	0.0011×10^8
Einsteins absorption probability: B_{nm}	1.25×10^8	1.43×10^8	1.17×10^8	1.21×10^8
Einsteins emission probability: A_{mn}	0.51×10^8	0.59×10^8	0.48×10^8	0.50×10^8

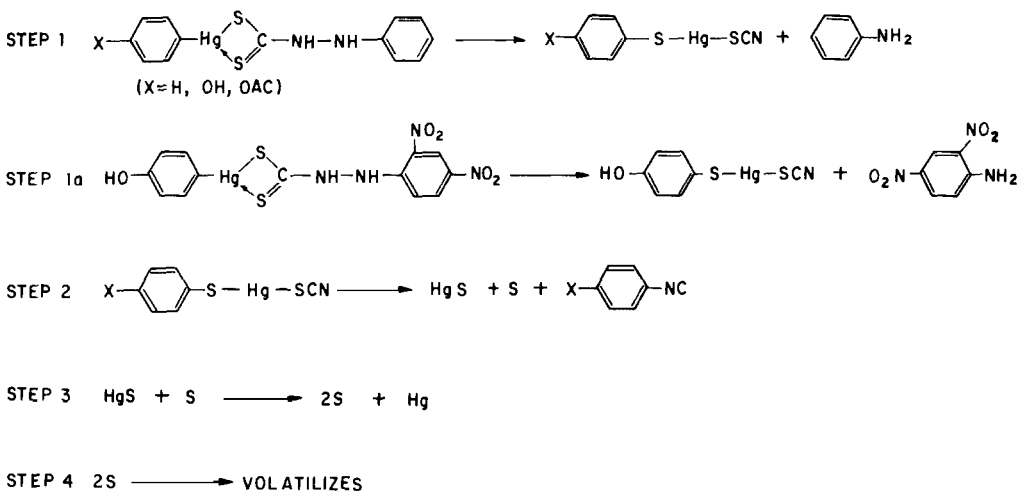

Scheme 1.

Thermal Studies

Thermogravimetric studies for C_6H_5HgL, *p*-HOC_6H_4HgL and *p*-$AcOC_6H_4HgL$ indicate that the thermal degradation is accomplished in four steps as shown in Scheme 1. For *p*-HOC_6H_4HgL', the degradation pattern is similar, except that 2,4-dinitroaniline is formed instead of aniline in step 1. In the final step, the elemental sulphur slowly volatilizes beyond 717 K. At 973 K, the volatilization is complete and the crucible of thermobalance is rendered empty. From the type of thermal effects on DTA curves, it is concluded that steps 1 and 4 are exothermic, while steps 2 and 3 are endothermic in nature.

From TG curves, the order (n) and activation energy (E_a) for steps 1 and 2 of the thermal reactions have been elucidated by the method of Coats and Redfern [23]. The sequence of E_a values reveals that the Ar–Hg bond is cleaved during thermal degradation as has been shown by our earlier studies [5]. The apparent activation entropy ($S^{\neq}$) for step 1 has been enumerated by the method of Zsako' [24]. From DTA curves, the change in enthalpy (ΔH) for the first thermal effect has been calculated in each case [25]. The temperature dependent calibration coefficient was obtained from the Currell equation [26]. The data are presented in Table III.

Mass Spectra

The fragmentation pattern of the complexes is shown in Scheme 2 (1)–(5). The RHg^+, R^+, $HgCl^+$ and Hg^+ ions dominate the mass spectra [27]. Fragmentation of the ligand portion, shown in Scheme (1), is common to all the complexes. The carbonium ion R^+, is the base peak for all the complexes. The fragmentation pattern of the complex with R = C_6H_5 eqn. (2) is consistent with the mass spectra of similar compounds [28]. The fragments from *p*-hydroxyphenyl complexes eqn. (3), were also observed in the spectra of corresponding *o*-hydroxyphenyl analogues [29]. In the case of *p*-acetoxyphenyl complexes eqn. (4) and furyl complexes eqn. (5), the cleavage of the C–O bond is a significant fragmentation mode [30].

Biochemical Studies

The C_6H_5HgL and C_6H_5HgL' complexes were screened against the two fungal species, *Aspergillus fumigatus and Aspergillus niger* at 25 μg/ml and 50 μg/ml concentrations. The results of antifungal inhibition were compared with standard drug babestein, which was also tested at the same concentrations. The complexes showed 45–70% inhibition. Better inhibition was observed at a lower concentration for C_6H_5HgL complex and at a higher concentration for C_6H_5HgL' complex. The order of activity is *A. fumigatus* > *A. niger*.

TABLE III. Kinetic and Thermodynamic Parameters from Thermal Studies

Compound	Step	n	E_a (kcal mol^{-1})	$S^{\neq}$ (e.u.)	ΔH (cal g^{-1})
C_6H_5HgL	1	1	6.10	4.12	9.90
	2	1	2.74	–	–
p-HOC_6H_4HgL	1	1	6.53	4.67	3.23
	2	1	3.43	–	–
p-$AcOC_6H_4HgL$	1	1	5.85	3.40	14.22
	2	1	2.37	–	–
p-HOC_6H_4HgL'	1	1	4.57	2.00	17.37
	2	1	3.35	–	–

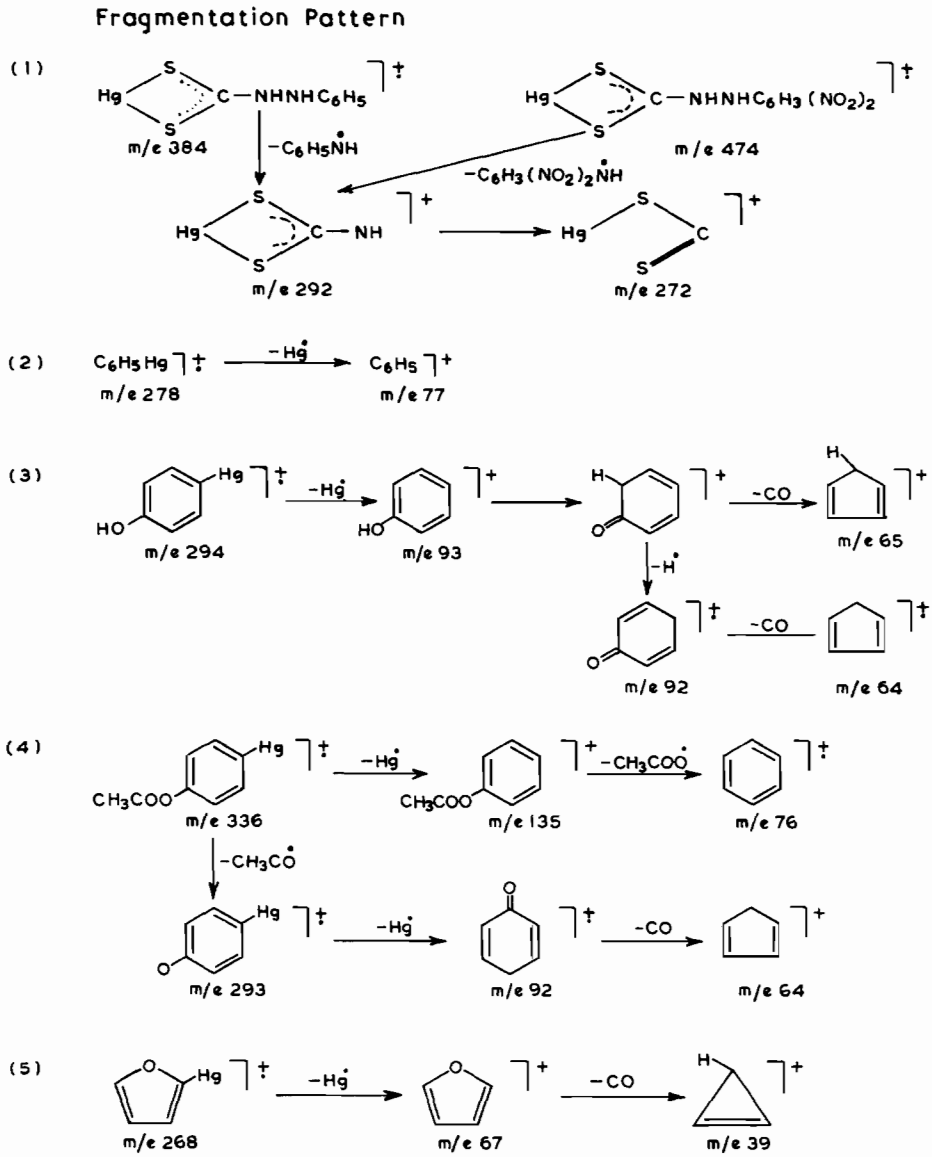

Scheme 2.

These complexes were also tested for antibacterial activity *in vitro*. The screening of the samples was carried out against two bacteria, *viz.* gram positive *Staphylococcus aureus* and gram negative *Escherichia coli* at two concentrations, *viz.* 50 μg/ml and 100 μg/ml. The compounds showed significant inhibition against both the bacterial strains. They were more active at higher concentrations. The order of activity against the two microorganisms is *S. aureus* > *E. coli*.

References

1 M. A. Ali and S. E. Livingstone, *Coord. Chem. Rev., 13,* 101 (1974).
2 M. Das and S. E. Livingstone, *Inorg. Chim. Acta, 19,* 5 (1976).
3 T. Glowisk and T. Ciszewska, *Inorg. Chim. Acta, 27,* 27 (1978).
4 G. S. Sodhi, R. K. Bajaj and N. K. Kaushik, *Inorg. Chim. Acta, 92,* L27 (1984).
5 S. Kamrah, G. S. Sodhi and N. K. Kaushik, *Inorg. Chim. Acta, 107,* 29 (1985).
6 R. C. Fay and R. N. Lowry, *Inorg. Chem., 6,* 1512 (1967).
7 U.S. Pat. 2502222 (1950) to J. F. Kaplan and C. Mellick; *Chem. Abstr., 44,* 6882 (1950).
8 F. C. Whitmore and E. R. Hanson, 'Organic Synthesis Coll.', Vol. I, Wiley, New York, 1932, p. 155.
9 F. C. Whitmore and E. B. Middleton, *J. Am. Chem. Soc., 43,* 619 (1921).
10 H. Gilman and G. F. Wright, *J. Am. Chem. Soc., 55,* 3302 (1933).
11 U. Anthoni, *Acta Chim. Scand., 23,* 2742 (1966).
12 B. B. Kaul and K. B. Pandeya, *J. Inorg. Nucl. Chem., 40,* 1035 (1978).

13 F. Bonati and R. Ugo, *J. Organomet. Chem., 10,* 257 (1967).
14 A. Braibanti, A. M. M. Lanfredi and A. Tiripicchio, *Acta Crystallogr., Sect. B, 25,* 93 (1969).
15 R. S. P. Coutts, P. C. Wailes and R. L. Martin, *J. Organomet. Chem., 50,* 145 (1973).
16 C. K. Jorgenson, *J. Inorg. Nucl. Chem., 24,* 1571 (1962).
17 C. A. Tsipis and G. E. Manoussakis, *Inorg. Chim. Acta, 18,* 35 (1976).
18 F. Takami, S. Wakahara and T. Maeda, *Tetrahedron Lett.,* 2645 (1971).
19 M. L. Janssen, *Recl. Trav. Chim., 79,* 1066 (1960).
20 E. J. Brown and F. Wokes, 'The Fluorescence of Solution', Longmans Green, London, 1953.
21 J. G. Calvert and J. N. Pitts, 'Photochemistry', Wiley, New York, 1966.
22 K. K. Rohtagi-Mukharjee, 'Fundamentals of Photochemistry', Wiley-Eastern, N. Delhi, 1978.
23 A. W. Coats and J. P. Redfern, *Nature (London), 201,* 68 (1964).
24 J. Zsako', *J. Phys. Chem., 72,* 240 (1968).
25 W. E. Collins, 'Analytical Calorimetry', Vol. 2, Plenum, New York, 1970.
26 B. R. Currell, 'Thermal Analysis', Vol. 2, Academic Press, New York, 1969.
27 F. Glockling, J. R. Irwin, R. J. Morrison and J. J. Sweeney, *Inorg. Chim. Acta, 19,* 267 (1976).
28 W. F. Bryant and T. H. Kinstle, *J. Organomet. Chem., 24,* 573 (1970).
29 T. Aczel and H. E. Lumpkin, *Anal. Chem., 32,* 1819 (1960).
30 D. H. Williams, R. G. Cooks, J. Ronayne and S. W. Tam, *Tetrahedron Lett.,* 1777 (1968).